PRELIMINARY FEASIBILITY ANALYSIS OF GPS IIIC INTEGRATED WITH AN INERTIAL SYSTEM TO PROVIDE CAT IIIB SERVICES*

Young C. Lee
Curtis A. Shively
Tan (Tyler) Zou
Center for Advanced Aviation System Development
The MITRE Corporation, McLean VA

BIOGRAPHIES

Dr. Young C. Lee is a member of the Principal Staff at the Center for Advanced Aviation System Development (CAASD) of the MITRE Corporation. He has been working in the area of GPS integrity since 1986 in support of the Federal Aviation Administration (FAA). He also has been serving as secretary of RTCA SC-159 and as co-chairman of its GPS/Inertial Working Group. He received his B.S. from Seoul National University in Korea and his Ph.D. from the University of Virginia, both in electrical engineering.

Curtis A. Shively is a member of the Principal Staff at MITRE/CAASD. He has studied the use of satellites for communications, navigation and surveillance. He received his B.S. and M.S. in Electrical Engineering from the Massachusetts Institute of Technology.

Tan (Tyler) Zou worked as an intern at MITRE/CAASD during the summer of 2009, when he participated in the analysis reported in this paper. He is currently a sophomore at Harvard University majoring in mathematics and computer science. He serves as the Chief Information Officer of Harvard Project for Asian and International Relations and was previously the Chief Technology Officer of the project.

ABSTRACT

This paper describes a preliminary analysis of the potential for an integrated GPS IIIC/inertial navigation system to provide Category IIIB (CAT IIIB) precision approach and landing services. The CAT IIIB landing requirements are expressed as restrictions on the vertical navigation sensor error (NSE) to ensure a high probability of safe landing under both fault-free and faulted conditions. In particular the most restrictive requirement dictates the probability of missed detection of a satellite range fault. The integrated system comprises a navigation grade inertial sensor tightly coupled with a GPS receiver, using pseudorange and delta range measurements to update the inertial measurements. GPS fault detection is performed by applying a threshold to the innovation residual (difference between predicted and measured ranges). A Monte Carlo simulation is used to estimate missed detection performance of the integrated system. Both step faults and ramp faults are considered. Results indicate that the integrated GPS IIIC/inertial system as modeled could likely meet the CAT IIIB fault detection requirements for any size step or ramp without even using delta range measurements.

INTRODUCTION

Many papers have previously been published on integrated GPS/inertial navigation systems to improve continuity and availability of service upon loss of GPS signals caused by intentional or unintentional GPS interference, occasional periods of poor user-to-satellite geometry or by ionospheric scintillation, for example [1, 2, 3]. However, almost all of these studies for GPS applications have focused on the capability required for en route through nonprecision approach. Recently with the expectation of much improved GPS performance in the future, interest has shifted to the feasibility of supporting more demanding navigation applications without external augmentations to GPS. As an example, the GNSS Evolutionary Architecture Study (GEAS) Panel evaluated a GPS-based architecture using absolute RAIM (ARAIM) to provide robust worldwide instrument approach guidance known as LPV-200 in the 2025–2030 timeframe [4, 5]. Modernized GPS will provide dual-frequency civil signal transmissions that will allow users

* The contents of this material reflect the views of the authors. Neither the Federal Aviation Administration nor the Department of Transportation makes any warranty or guarantee, or promise, expressed or implied concerning the content or accuracy of the views expressed herein.

to virtually eliminate errors resulting from un-modeled ionosphere delay, currently the largest source of range error in single-frequency GPS. In addition, modernized GPS will rely on enhanced ground segment monitoring and processing to decrease satellite ephemeris and clock estimation errors. As a result, a significant improvement in signal-in-space (SIS) accuracy is expected. In particular, modernized GPS in its end state will provide integrity assurance. GPS III satellites (GPS IIIC) will be equipped with built-in capabilities to detect clock failures and other on-board hardware/software faults. Also, the GPS III control segment will be designed to validate commands and uploads before they are transmitted to the satellites, thereby ensuring a much reduced probability of signal-in-space faults. According to the current GPS III Specifications, if the instantaneous User Range Error (URE) exceeds 5.73 times the broadcast URA value, the signal will be removed (switched to non-standard code) within 5.2 sec with a very high probability [6].

The current study explores the possibility of providing CAT IIIB by relying on an integrated GPS/inertial technology taking advantage of GPS III capability. Integrated GPS/inertial system performance has already been evaluated for RNP operations, including lateral guidance for nonprecision approaches. The CAT IIIB landing requirements are much more demanding because they include precision approaches with vertical guidance for touchdown on the runway. As in most GNSS-based systems, the major issue is not so much accuracy but integrity and its availability. While the accuracy that can be provided with GPS IIIC alone might meet the CAT IIIB requirements with adequate availability, the integrity requirements could not be met without an inertial integration, as this study shows. Using the range measurements from GPS IIIC to calibrate the inertial system would provide improved accuracy and integrity. However, GPS IIIC SIS integrity performance is constrained by a 5.2 sec time-to-alert, while CAT IIIB operations require a time-to-alert of 2 sec or less. Also the accuracy and integrity performance provided by GPS IIIC may not be sufficient to meet the CAT IIIB requirements. This gap in the requirements may be filled by augmenting GPS IIIC with an inertial system. Since the vertical channel of an inertial system is typically quite stable over short periods of time, it is expected that there will be no significant inertial error growth during a short delay time. For this reason, a vertical position error is directly estimated in the Kalman filter rather than using the baro-inertial altimeter that has traditionally been used.

The purpose of this study is to evaluate the feasibility in the GPS IIIC time frame of using a GPS receiver integrated with a navigation grade inertial system in the avionics to provide robust CAT IIIB service worldwide. GPS III will be implemented in phases progressing from less capable GPS IIIA to GPS IIIC, the most capable in terms of accuracy and integrity. This preliminary study starts with GPS IIIC because it provides the best chance to achieve CAT IIIB performance. The work will continue with less capable GPS III once the feasibility of the concept has been shown with GPS IIIC. Another significant benefit of inertial integration is the ability to provide backup capability for GPS, which would address one of the FAA's primary concerns. For this reason, this study will also be extended to evaluate coasting capability possible with GPS III for various service levels. The ultimate goal of this analysis is to support a future NextGen decision on PNT infrastructure and backup.

The paper has three main sections. In the next section, the CAT IIIB navigation system error (NSE) requirements are reviewed. Then, the expected integrity performance of GPS III alone is estimated. The analysis leads to the conclusion that a stand-alone GPS receiver would not achieve CAT IIIB integrity performance with acceptable availability even in the GPS IIIC timeframe. The following section describes the GPS/inertial system architecture used for the performance analysis. It is followed by a section describing the performance evaluation. The performance evaluation focuses on integrity performance, namely, fault detection (or equivalently missed detection). The evaluation of missed detection probability (P_{md}) relies on a Monte-Carlo simulation. In this section, the assumptions of the simulation and the fault-free and faulted performance evaluation methodologies are described, and then the results are presented. The paper concludes with a summary and a discussion of future work. Three appendices are included at the end of the paper to provide further detail on some technical aspects of the discussion in the main body.

CAT IIIB NSE REQUIREMENTS

Category IIIB (CAT IIIB) operations encompass not only precision approach, but also landing and rollout. Therefore, the performance requirements for CAT IIIB are expressed in terms of probability of a safe landing as represented by the touchdown point of the aircraft on the runway. The touchdown point is related to the total system error (*TSE*), which is modeled as the sum of two components: 1) flight technical error (*FTE*) related to the aircraft landing system's attempt to achieve the desired path and 2) navigation sensor error (*NSE*) related to the estimate of the aircraft's actual position. Consideration must of course be given to landing performance in both the lateral and longitudinal dimensions. For this type of performance analysis, the longitudinal touchdown performance is often assumed to have a simple linear relationship to the vertical *NSE* (NSE_V). Furthermore, it is also commonly recognized that safe landing places more stringent requirements on vertical *NSE* than on lateral

NSE. Therefore, only the longitudinal dimension for *TSE* (vertical dimension for *NSE*) will be considered herein.

The safe landing requirements addressed in this paper were developed for achieving CAT IIIB performance using a ground-based augmentation system (GBAS) with GPS. A new terminology has been adopted under which this capability is referred to as GBAS Approach Service Type D (GAST D). The technical concept for GAST D is extensively described in various papers including [7]. The GAST D concept meets NSE performance requirements formulated to address three circumstances: 1) fault-free nominal condition, 2) faulted limit case, and 3) faulted malfunction case. Thorough derivations and discussions of these requirements, particularly the two faulted cases, have been presented previously in several sources, including [7–11]. For the convenience of the reader, the derivations and assumptions used in this analysis are summarized in Appendix A. Only a brief description and the results are presented immediately below.

Nominal Condition. Under fault-free conditions the probability of unsafe landing must not exceed 10^{-6}. Given assumptions for *FTE* and the approach glide path angle (*GPA*), this requirement restricts the standard deviation of a Normal distribution characterizing NSE_V

$$\sigma_{NSE_{V,\,fault-free}} \leq 2.38\,\mathrm{m} = 7.82\,\mathrm{ft} \tag{1}$$

Limit Case. Given that a fault is present, the probability of unsafe landing must not exceed 10^{-5}. This requirement places a restriction on the probability of missed detection (P_{md}) of the vertical error bias produced by the fault, $NSE_{V,fault\text{-}bias}$. The resulting P_{md} restriction is shown in Figure 1. Note that the allowable P_{md} increases for decreasing vertical bias values and may be as large as 1.0 (never detected) for $NSE_{V,fault\text{-}bias}$ smaller than about 1.8 m.

Malfunction Case. For faults more likely than 10^{-9}, the landing must be safe with complete certainty (probability 1.0). Since the malfunction case includes the prior probability of fault, P_{fault}, the product of P_{fault} and P_{md} must not exceed 10^{-9} for any fault larger than the particular value, $E_{V\_safe\_max}$, that would make the landing unsafe. For the assumptions in this analysis $E_{V\_safe\_max}$ = 7.2 m (See Appendix A). Thus, an equivalent restriction inversely proportional to P_{fault} is placed on P_{md} for any value of $NSE_{V,fault\text{-}bias}$ larger than 7.2 m. The resulting P_{md} restriction for several values of $P_{fault\_per\_hour}$ is also shown in Figure 1. (See Appendix A for the relationship between P_{fault} and $P_{fault\_per\_hour}$.) Note, for example that for $P_{fault\_per\_hour}$ = 10^{-4} to 10^{-5} there is a region of $NSE_{V,fault\text{-}bias}$ where the malfunction case requirement is more restrictive than the limit case requirement. However, for $P_{fault\_per\_hour}$ = 10^{-6}, the malfunction case requirement has no effect.

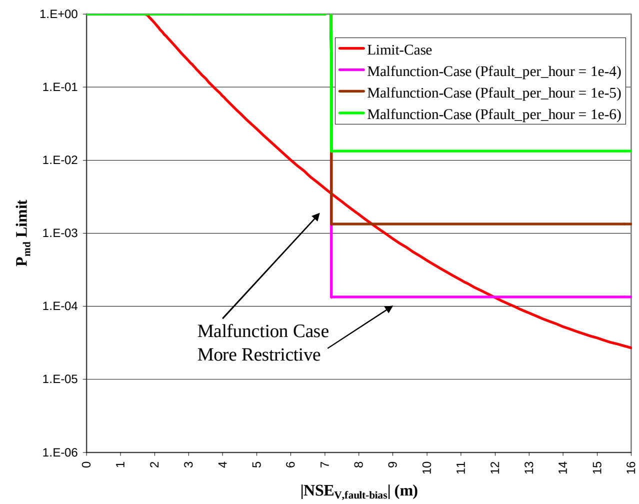

Figure 1. P_{md} Limit versus $NSE_{V,fault\text{-}bias}$ for Limit Case and Malfunction Case

INTEGRITY PERFORMANCE OF GPS III ALONE

The performance standards for GPS III are currently under development and not finalized. Moreover, the first GPS IIIC satellites are not anticipated to be launched until around the year 2019. Consequently, only limited and somewhat uncertain information on the integrity capability of GPS IIIC is available, especially in the public domain [6]. However, a basic characterization of desired GPS IIIC integrity performance is known. GPS satellites broadcast a user range accuracy (*URA*) parameter. For GPS IIIC, if the integrity status flag is set to 'on', the user is assured that the probability the satellite range error (*URE*) exceeds 5.73×*URA* without notification within 5.2 sec is limited to 10^{-8} per hour. A second performance requirement has also been established for 4.42 × *URA* with the corresponding probability 10^{-5} per hour, which should apply whether the integrity status flag is 'on' or 'off'. Note that the above factors and probabilities suggest that the errors follow a Normal distribution with standard deviation equal to *URA*. However, the draft GPS III specifications do not guarantee that *URE* will be normally distributed with standard deviation equal to *URA*. Moreover, for the purpose of comparison to CAT IIIB *NSE* requirements in the faulted circumstance (e.g., Figure 1), a "monitor" with appropriate missed detection probability characteristic is needed. Since no such "monitor" characteristic has been documented (at least in the public domain) for integrity-assured GPS IIIC, a notional P_{md} vs $E_{V,fault\text{-}bias}$ curve will be inferred using the following rationale.

The 10^{-8} per hour probability at $5.73 \times URA$ is the product of a prior probability of fault and the P_{md} at $5.73 \times URA$. Assuming a prior probability of fault = 10^{-4} per hour and URA = 0.5 m gives P_{md} (2.87 m) = 10^{-4}. The monitor threshold can be expressed as $T_{mon} = K_{fd} \times \sigma_{mon}$. Assuming a probability of false detection on the order of 10^{-10} and Normally distributed monitor decision statistic gives K_{fd} = 6.47. The additional "buffer" for $P_{md} = 10^{-4}$ is $3.27 \times \sigma_{mon}$. Thus, $(6.47 + 3.27) \times \sigma_{mon}$ = 2.87 m, or σ_{mon} = 0.28 m and T_{mon} = 1.82 m.

Figure 2 shows a graph comparing this notional inferred P_{md} characteristic for integrity-assured GPS IIIC to the P_{md} requirements for CAT IIIB. It should be pointed out that the GPS IIIC performance is characterized for a single satellite in the range domain, but CAT IIIB required P_{md} performance is inherently characterized in vertical position. Therefore, in order to make a comparison, an assumption must be made for the value of S_{vert}, the coefficient in the position solution that transforms range error for an individual satellite into vertical position error. Consequently, Figure 2 shows four curves for the CAT IIIB P_{md} requirement expressed in the range domain assuming S_{vert} = 1, 2, 3, or 4. Note that in order for the notional GPS IIIC P_{md} performance to be satisfactory, S_{vert} would need to be restricted to a value of approximately 1.3. Restrictions of S_{vert} to approximately 4 or less have already been proposed for use in GAST D to limit undetected error due to ionospheric anomalies [12]. However, as part of the GAST D analysis it was recognized that restricting S_{vert} to be any smaller than about 3.0 can significantly lower availability of satellite geometry [12, 13]. Thus, it is unlikely that GPS IIIC could achieve CAT IIIB integrity performance with acceptable availability.

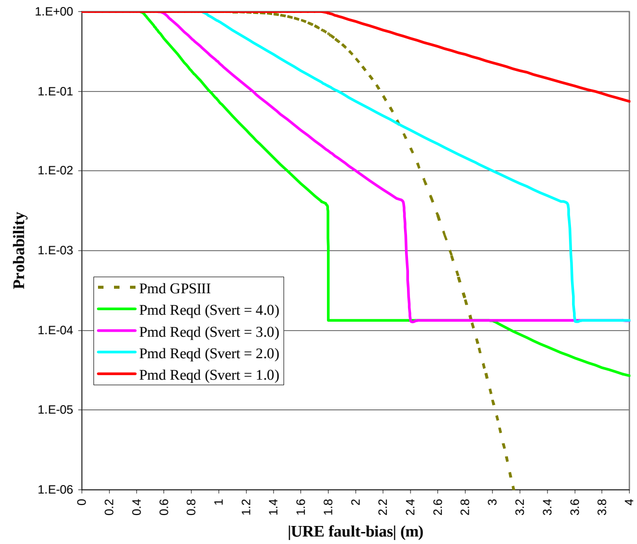

Figure 2. Notional P_{md} Performance of GPS IIIC Compared to CAT IIIB Requirement

GPS/INERTIAL SYSTEM ARCHITECTURE

The system architecture used as the basis of our simulation model is a tightly coupled GPS/inertial system described in detail in [14] and illustrated in Figure 3. As shown, the system consists of three units: a GPS receiver, an Inertial Reference System (IRS), and an integration processor (IP). The IRS generates inertial solutions in an *open loop* mode and passes the information to the IP. The GPS receiver generates the pseudorange (PR) measurements and satellite positions and passes these measurements to the IP. Using these inputs from the GPS receiver and the IRS, the IP generates corrections to the IRS solutions using a Kalman filter.

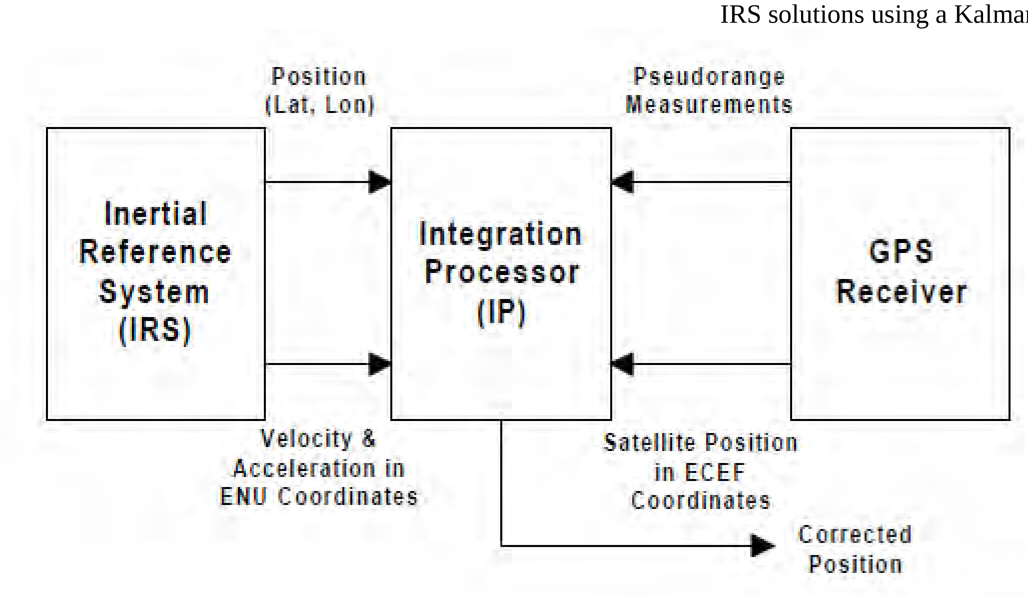

Figure 3. System Architecture for a Tightly Coupled GPS/Inertial System

A navigation grade inertial sensor is assumed for the IRS and a good quality temperature-controlled crystal oscillator clock is assumed for the GPS receiver [3]. The measurements used by the Kalman filter are two types of range measurements from the satellites: PRs and delta PRs, where the latter are the PR rates of changes taken from the carrier tracking loop. Each PR measurement in the measurement vector is derived from the difference between two PRs to each satellite. One is the measured PR input from the GPS receiver. The other is the PR computed on the basis of the satellite positions obtained from the GPS receiver and the user location output by the IRS. Likewise, each delta PR measurement in the measurement vector is similarly derived from the difference between the measured and computed delta PRs. Using this measurement vector, the IP calculates the corrections to the inertial solutions and provides estimates of the integrity of the corrected solutions. The IP first processes the measurement vector at a 1 Hz rate and pre-filters the data every 10 sec interval. The data are then passed to the Kalman filter. With pre-filtering, most of the high frequency components in the measurements are assumed to be removed. The remaining components of the measurements are modeled as satellite bias errors. A total of 24 error states are defined for the Kalman filter as shown in Table 1.

Table 1. Error States for the Kalman Filter

IRS Error States	$d\theta_x$, $d\theta_y$, $d\theta_z$	Horizontal angular position errors
	dh	Vertical position error
	dV_x, dV_y, dV_z	Linear velocity errors
	$d\phi_x$, $d\phi_y$, $d\phi_z$	Navigation axis misalignments
	dGB_x, dGB_y, dGB_z	Gyro bias errors
	dAB_x, dAB_y, dAB_z	Accelerometer bias errors
User clock Error States	dB	User clock bias
	dBr	User clock bias rate
Satellite Range Bias Error States	dRB_i (i = 1, 2, … N)	Satellite i range bias error (N = 6)

It is assumed in this paper that range measurements from the satellites are either PRs only or both PRs and delta PRs taken from the carrier tracking loop. In general, use of delta PRs can greatly improve performance, but it also leads to a more difficult implementation. For example, it requires a precise lever arm correction, and an attention should be paid to possible cycle slips. For this reason and also because CAT IIIB requirements are met using pseudorange measurements alone, the results are shown only for that case.

PERFORMANCE EVALUATION

Conditions for Simulation

Flight profile

A 60-min long flight is assumed which includes two 180-deg turns, one at the beginning of the flight and the other at the end, immediately before a presumed landing. In general, GPS/inertial performance heavily depends on the timing of the flight maneuvers relative to the time of loss of GPS signals when this results in a relatively long period of coasting (without GPS calibration). In the current study it is assumed that GPS measurements are available continuously, but the Kalman filter processes them at every update interval of 10 sec, and the position solution integrity is evaluated for a minute. Over such a short duration, the error growth in the vertical channel of an inertial system is negligible, and the performance would not be affected by the flight maneuver.

User location

A single location in the conterminous United States is assumed.

Satellites

The nominal 24-satellite GPS constellation is assumed. Over the flight duration, different satellites are in view of the user. Out of those, six satellites are visible to the user continuously throughout the flight. For the sake of simplicity, only these satellites are used as ranging sources by the simulation. VDOP varies between 1.6 and 2.2 and HDOP between 1.1 and 1.3 during the flight.

Satellite range measurements

Two cases are considered: one in which only PR is used, and the other in which both PR and delta PR taken from the carrier tracking loop (velocity) are used.

Assumptions on range measurement accuracy

Two parameters are defined regarding the range measurement errors: one characterizes the measurement noise and the other, the process noise for the range bias error states. Both of these errors are assumed to have Gaussian distribution with a zero mean. The standard deviations are assumed as follows.

For the PR measurement, the standard deviation of high frequency satellite range error averaged over the Kalman Filter update cycle ($\sqrt{R_k}$) was selected on the basis of the user range error model and URE of 0.25 m that were previously assumed by the GEAS [4, 5]. Since the user error varies as a function of satellite elevation angle, and thus as a function of time, $\sqrt{R_k}$ varies as a function of time. A typical $\sqrt{R_k}$ value of 0.5 m is observed. $\sqrt{R_k}$ for delta PR taken from the carrier tracking loop was selected as 0.5 cm/sec.

The range bias error is assumed to have a 1-hour correlation time constant, and the value of its standard deviation ($\sqrt{Q_k}$) was selected as 0.1 m, the same value selected by the GEAS for the nominal bias magnitude [4, 5].

As noted earlier, CAT IIIB requirements are more stringent for vertical *NSE* than for lateral *NSE*. Therefore, in our analysis, the focus has been placed on the vertical position error performance.

Fault-Free Performance

Figure 4 shows the simulation results of the vertical position error in the absence of a fault over the flight duration of 60 min (without using delta PR). It also shows one standard deviation of the error over the same duration. As the figure shows, the standard deviation quickly converges at the beginning and continues to decrease slowly thereafter. The simulated error also tends to decrease as time passes. The flight profile has a 180 deg turn immediately before the end, and yet no appreciable jump in either standard deviation or position error is observed. This is because the GPS range measurements are available continuously.

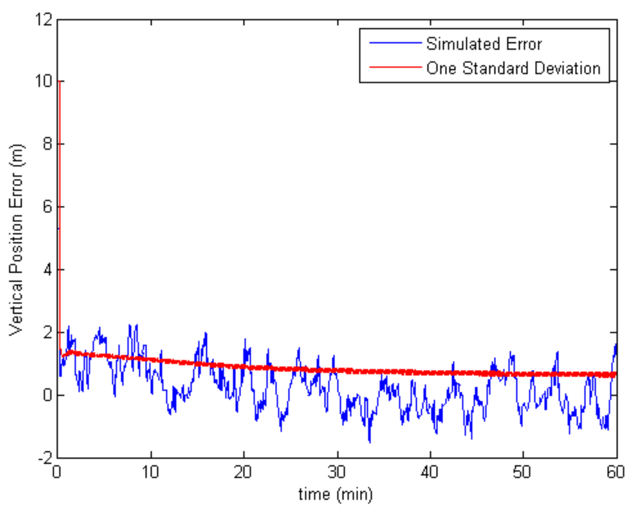

Figure 4. Variation of Simulated Vertical Position Error in the Absence of a Fault

Faulted Performance

In this study, integrity performance is evaluated via a Monte Carlo analysis to determine the probability of missed detection (P_{md}) in the presence of a fault. It is assumed that a fault may cause one of two types of errors: ramp error or step error. Errors of each of these types with different magnitudes and signs are introduced at the most critical time, namely when the aircraft begins to turn immediately before landing. With these errors introduced in the measurements, the resulting test statistics and the vertical position errors are calculated and the missed detection events are counted.

Introduction of a fault

Faults (ramps or steps) of various sizes are introduced into the measurements one satellite at a time and the fault size that causes the largest P_{md} is determined for each vertical error threshold. It is assumed that the ramp error starts exactly at a Kalman filter update time and the step error starts midway between two successive update times. Different times could have been assumed, but it is believed that the results would not be significantly different if different times had been selected.

Effect of a fault on measurement vector

The effect of a fault on the measurement vector depends on the type of range measurement (PR or delta PR) and the type of fault (ramp or step). In case there are N satellites and only PR measurements are used, the length of the measurement vector is N. In case delta PRs are used, the measurement vector has N additional elements for the delta PRs. Therefore, when the j^{th} satellite is assumed to have a fault, the resulting range error affects the j^{th} element of the measurement vector and the velocity error affects the $(j+N)^{th}$ element. The effect of a fault is simulated in the Kalman filter by averaging the bias errors in the PRs (and, if applicable, in the delta PRs) caused by the fault over each Kalman filter cycle and adding them to the nominal random errors in the measurement vector. This is further explained by an illustration in Appendix B.

Fault detection scheme

For fault detection, a scheme that was originally proposed by Dr. John Diesel of Litton for his AIME algorithm is used in this paper. The scheme, which is described in detail in [15], uses the normalized innovation residual, which was shown to have a chi-square distribution, central in the absence of a fault and non-central in the presence of a fault. The detection threshold is determined from the central chi-square distribution on the basis of the maximum allowable false detection probability. Following the methodology proposed for AIME, this paper calculates six test statistics at each Kalman filter update time. One test static is obtained by averaging the normalized innovation residuals over the past N Kalman filter update cycles where N = 1, 2, … 6. This is done to maximize the detection capability to catch a fault causing a slowly increasing error. If any of the multiple test statistics exceeds the detection threshold, a fault detection is declared. The detection threshold is determined conservatively by assuming that the multiple test statistics are all independent.

P_{md} Evaluation methodology

While test statistics are calculated at each Kalman filter update time (t_k), the position error that results from ramp or step errors combined with random range errors is calculated every receiver processing time interval (assumed to be every second). The position error between Kalman filter update times is extrapolated from the last position update and the last vertical velocity estimate as

$$\tilde{h}(t) = \tilde{h}(t_k) + \tilde{V}_z(t_k)\cdot(t - t_k) \quad \text{for } t_k \le t < t_{k+1} \qquad (2)$$

where t_k is the k^{th} Kalman filter update time, and $\tilde{h}(t)$ and $\tilde{V}_z(t)$ denote the vertical position and velocity errors, respectively at time t.

Depending on the fault detection result and the size of the position error relative to the position error threshold (Ev), one of four possible outcomes is declared: missed detection, early detection, timely detection, or no event. In the determination of the outcome, the 2-sec time-to-alert allowed for CAT IIIB operations is taken into consideration as illustrated in Figure 5.

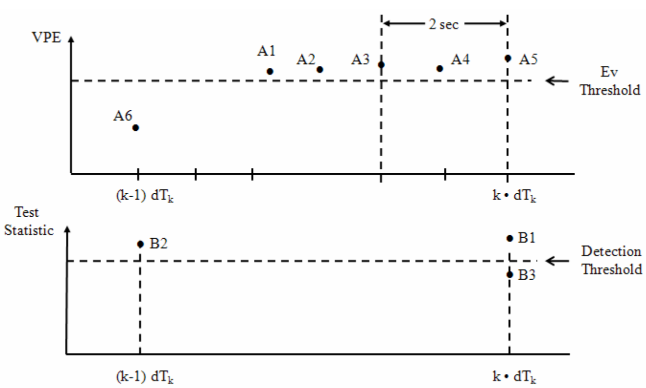

Figure 5. Timeline of Events Showing Whether or Not a Missed Detection Occurs

The figure shows the timeline of events in terms of vertical position error as compared to the Ev threshold (upper panel) and the test statistic (in this case, the largest of the multiple test statistics) as compared to the detection threshold (lower panel). A missed detection occurs when the position error exceeds the Ev threshold at any time during the previous Kalman filter update cycle and the test statistic is below the detection threshold at k·dTk (e.g., B3 with A1-A5). A missed detection also occurs even when the test statistic exceeds the detection threshold if the position error exceeding the Ev threshold occurred more than 2 sec before k·dTk (e.g., B1 with A1-A2). A timely detection occurs with B1 occurring with A3, A4, or A5.

Duration of P_{md} evaluation

It was mentioned above that a fault is introduced when the aircraft begins to turn immediately before landing. It is pointed out here that P_{md} is evaluated only for a duration of one minute after the fault is introduced because it is believed that P_{md} would be the worst during this period. It is also believed that a faulty satellite would be removed by GPS IIIC within a minute.

Vertical Protection Level (VPL)

VPL is formulated by extending the HPL formula developed for AIME by Dr. John Diesel [14, 15]. This is described in Appendix C. The value of VPL for the time at which P_{md} is evaluated is compared with the simulation results below.

Variation of P_{md} as a function of error size

Figure 6 shows P_{md} as a function of ramp slope for a few different vertical error thresholds. As the figure shows, for any given vertical error threshold, P_{md} varies widely and the peak occurs at slightly different slopes for different vertical error thresholds. Similar plots were obtained for P_{md} as a function of step error size.

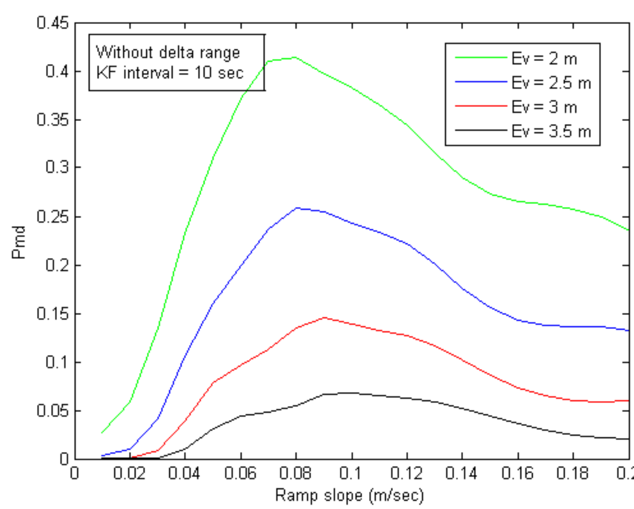

Figure 6. Probability of Missed Detection as a Function of Ramp Slope (Without Delta PR)

P_{md} Observed versus P_{md} requirements as a function of vertical error threshold

From plots like Figure 6, the largest P_{md} value is taken for each error threshold and plotted against the CAT IIIB requirements. The resulting P_{md} values without using delta PR are shown as a function of the error threshold in Figures 7 and 8. Note that the malfunction case requirement varies with the prior probability of fault per hour. A value of 10^{-4} applies for step faults and a value of 10^{-6} applies for ramp faults [16]. Figures 7 and 8 are for ramp and step faults, respectively.

The figures show that even the maximum P_{md} meets all the P_{md} requirements consistently for both types of errors without using delta PR. Furthermore, P_{md} performance is almost the same for ramp and step errors. Also shown is the VPL corresponding to P_{md} of 0.001 at the time the Monte-Carlo simulation was performed. It is shown that the VPL derived by extending the AIME HPL formula does not meet the CAT IIIB requirement. However, this AIME HPL formula is quite conservative.

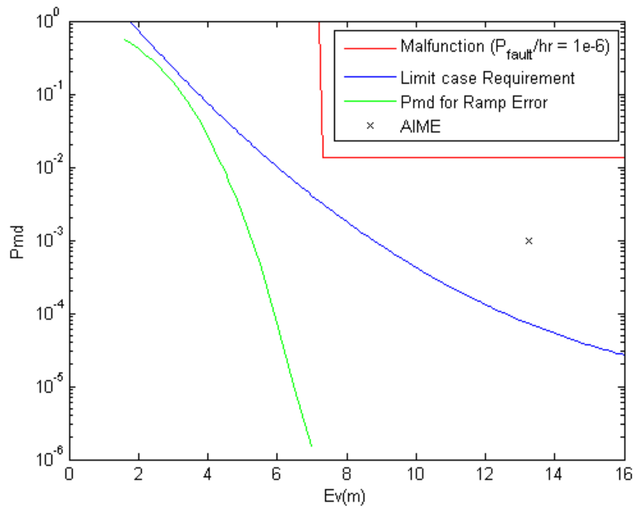

Figure 7. Observed P_{md} for Ramp Faults vs. P_{md} Requirements (Without Delta PR)

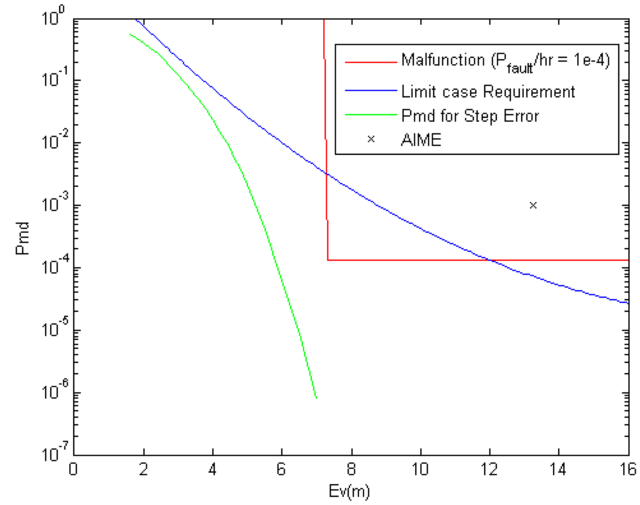

Figure 8. Observed P_{md} for Step Faults vs. P_{md} Requirements (Without Delta PR)

SUMMARY

The study evaluated the performance of a GPS receiver integrated with a navigation grade inertial system in the GPS IIIC timeframe to determine if CAT IIIB requirements can be met. The evaluation was done using a Monte-Carlo simulation:

- For derivation of the test statistic for fault detection, a formula similar to one originally developed for AIME was used. To maximize detection capability, especially for slowly increasing errors, six test statistics are derived by normalizing the average of the innovation sequence over the previous one to six 10-sec Kalman filter update cycles. Each of these test statistics has a chi-square distribution, central in the absence of a fault and non-central in the presence of a fault.

- It was assumed that a fault would cause either a ramp error or a step error. These types of errors with varying magnitudes and signs were introduced in the measurements and the resulting test statistics and the vertical position errors were calculated. A missed detection was defined to be an event in which the vertical position error (Ev) exceeds a specified error threshold and yet no detection flag is raised within 2 sec. It was shown that for any given vertical error threshold, the probability of missed detection (P_{md}) evaluated via Monte Carlo analysis varies widely as a function of fault size. Out of those values, the largest P_{md} was taken for each error threshold. The largest P_{md} values were plotted as a function of the error threshold and compared to the CAT IIIB requirements.

- The results obtained showed that even without using delta PR measurements taken from the carrier tracking loop, GPS IIIC integrated with a navigation grade inertial system could likely meet the CAT IIIB integrity performance requirements.

- The results were obtained with a flight profile involving two 180 deg turns, one at the beginning of the flight and the other toward the end, for a single location, and using six satellites visible to the user throughout the flight. While this flight profile does not involve a great variety of conditions, it is believed to be adequate to ensure representative results. For this reason, it was surmised that, in the GPS IIIC timeframe, a GPS receiver integrated with a navigation grade inertial system could meet the CAT IIIB integrity performance with acceptable availability.

FUTURE WORK

The current preliminary study of a GPS receiver integrated with an inertial system to provide the CAT IIIB services in the GPSIIIC timeframe has yielded some promising results regarding its feasibility. However, the study will be expanded to address a number of issues, in particular:

- The study analyzed the integrity performance via Monte Carlo simulation. The protection level formula needed for the analysis was derived by extending the formula for AIME HPL. However, the resulting formula seems to be quite conservative and may thus have a negative impact on availability. An attempt should be made at developing a formula that provides a tighter protection level.

- The study has focused on integrity, that is, on the ability to detect a fault before it affects the integrity of the vertical position. That may be adequate for CAT IIIB operations. However, if it is desired to start using the integrated GPS/inertial system long before a CAT IIIB operation is initiated, it would be necessary to not only detect but also isolate a fault in order to ensure continued navigation. Such a capability would be particularly useful as a backup to GPS IIIC (for airframes equipped with inertial systems). The current study will be expanded to examine the feasibility of providing such a capability.

- The current study assumed signal-in-space range errors characterized by URE of 0.25 m (one standard deviation) following the similar assumption made by GEAS [4, 5]. However, the current GPS III specification does not guarantee that URE will always be at that level. Rather it merely states that, if the instantaneous User Range Error (URE) exceeds 5.73 times the broadcast URA value, the signal will be removed (switched to non-standard code) within 5.2 sec, where URA is specified to be less than or equal to 0.7 m with 0.9999 probability. This statement would allow the URE to sometimes be large. A follow-on study will evaluate the effect of URE larger than 0.25 m. Any other means of compensating for the negative impact of potentially larger errors will be explored such as use of delta PR measurements taken from the carrier tracking loop and a much higher quality user receiver clock.

APPENDIX A: DERIVATION OF CAT IIIB NSE REQUIREMENTS

This appendix summarizes the derivation of CAT IIIB navigation sensor error (NSE) performance requirements assumed for the analysis. More detailed derivations have been previously presented in several papers including [7-11]. NSE performance requirements are based on safe landing of the aircraft as determined by touchdown point on the runway. Performance in only the longitudinal dimension is considered because it is more difficult to achieve than in the lateral dimension.

For a safe landing the longitudinal touchdown point must be at least 200 ft past the runway threshold. The actual touchdown point depends on the total system error (*TSE*), modeled as the sum of longitudinal *NSE* (NSE_L) and aircraft flight technical error (*FTE*). *FTE* is assumed to be normally distributed with standard deviation σ_{FTE} about a nominal touchdown point *NTDP*. For this analysis *NTDP* = 1,275 ft and σ_{FTE} = 170 ft [10, 17]. A simple relationship is assumed between NSE_L and the vertical *NSE* (NSE_V) [8]

$$NSE_L = \frac{NSE_V}{\tan(GPA)} \tag{A-1}$$

For this analysis the glide path angle (*GPA*) is assumed to be 3.0 deg.

Three types of safe landing requirements have been applied to CAT IIIB guidance based on satellite navigation systems [8, 11]: 1) fault-free nominal condition, 2) faulted limit case and 3) faulted malfunction case.

Nominal Condition

For the nominal condition the probability of unsafe landing must not exceed 10^{-6}. Given assumptions for *FTE* and *GPA*, a resulting restriction on the standard deviation of $NSE_{V,fault\text{-}free}$ can be derived as follows

$$\text{Prob}\left\{\begin{array}{l}\dfrac{NSE_{V,fault\text{-}free}}{\tan[GPA]}\\ +FTE+NTDP\le 200\end{array}\right\}\le 10^{-6} \quad \text{(A-2)}$$

$$\begin{array}{l} NTDP \\ -4.753\times\sqrt{\left(\dfrac{\sigma_{NSE_{V,\,fault-free}}}{\tan[GPA]}\right)^2+\sigma_{FTE}^2} \\ \ge 200\end{array} \quad \text{(A-3)}$$

$$\begin{array}{l}\sigma_{NSE_{V,\,fault-free}} \\ \le \tan[GPA]\times\sqrt{\left(\dfrac{NTDP-200}{4.753}\right)^2-\sigma_{FTE}^2}\end{array} \quad \text{(A-4)}$$

For the assumptions used in the analysis

$$\sigma_{NSE_{V,\,fault-free}} \le 2.38\,\text{m} = 7.82\,\text{ft} \quad \text{(A-5)}$$

Limit Case

For the limit case, the conditional probability of unsafe landing given a fault occurs must not exceed 10^{-5}. The fault is assumed to add a bias ($NSE_{V,fault\text{-}bias}$) to the nominal NSE_V error distribution. The probability of unsafe landing is the product of the probability of missed detection of the fault bias and the probability the landing is unsafe given the fault bias is present

$$\begin{array}{l} Risk_{|\,fault} = P_{md}\left[NSE_{V,\,fault-bias}\right] \\ \times P_{UL}\left[NSE_{V,\,fault-bias}\right]\end{array} \quad \text{(A-6)}$$

The resulting constraint on P_{md} is calculated as follows

$$\begin{array}{l} P_{md}\left[NSE_{V,\,fault-bias}\right] \\ \le \min\left[1,\dfrac{10^{-5}}{P_{UL}\left[NSE_{V,\,fault-bias}\right]}\right]\end{array} \quad \text{(A-7)}$$

$$\begin{array}{l} P_{UL}\left[NSE_{V,\,fault-bias}\right] \\ = \text{Prob}\left\{\begin{array}{l}\dfrac{NSE_{V,\,fault-free}-NSE_{V,\,fault-bias}}{\tan[GPA]} \\ +FTE+NTDP\le 200\end{array}\right\} \\ = \displaystyle\int_{-\infty}^{200} dnorm\left[\begin{array}{l} x, \dfrac{-NSE_{V,\,fault-free}}{\tan[GPA]} \\ +NTDP, \sigma_{TSE}\end{array}\right]dx \end{array} \quad \text{(A-8)}$$

Where *dnorm[x,μ,σ]* is the Gaussian probability density function and

$$\begin{array}{l}\sigma_{TSE} = \sqrt{\left(\dfrac{\sigma_{NSE_{V,\,fault-free}}}{\tan[GPA]}\right)^2+\sigma_{FTE}^2} \\ = \sqrt{\left(\dfrac{7.82}{0.0524}\right)^2+170^2} = 226\,\text{ft}\end{array} \quad \text{(A-9)}$$

Malfunction Case

For the malfunction case the landing must be safe with complete certainty (probability 1.0) for any fault condition that is more likely than 10^{-9}. A corresponding limitation on the product of the probability of fault during the exposure interval (P_{fault}) and the probability of missed detection is

$$\begin{array}{l} P_{fault}\times P_{\text{md}}\left[NSE_{V,\,fault-bias}\right] \\ \begin{cases}\le 10^{-9} \text{ if } NSE_{V,\,fault-bias} > \left|E_{V\_safe\_\max}\right| \\ \le 1.0 \text{ if } NSE_{V,\,fault-bias} \le \left|E_{V\_safe\_\max}\right|\end{cases}\end{array} \quad \text{(A-10)}$$

Where $E_{V\_safe\_max}$ is the largest fault bias for which the landing can be safe. The values of $NSE_{V,fault\text{-}free}$ and FTE are fixed at representative (95%) values [17]. Therefore, it is possible to determine $E_{V\_safe\_max}$ from

$$\begin{array}{l}\dfrac{-1.96\times\sigma_{NSE_{V,\,fault-free}}-E_{V\_safe\_\max}}{\tan[GPA]} \\ +NTDP-1.96\times\sigma_{FTE} = 200\end{array} \quad \text{(A-11)}$$

Solving (A-11) for $E_{V\_safe\_max}$ and substituting assumed or derived values for other quantities gives

$$E_{V\_safe\_\max} = 7.2\,\text{m} \quad \text{(A-12)}$$

Assuming, an exposure time of 15 seconds and a maximum of 18 ranging sources, the value of P_{fault} is determined as a function of the fault rate per hour

$$P_{\mathrm{fault}} = \frac{P_{fault\_per\_hr} \times 15 \times 18}{3600} = 7.5\times10^{-2} \times P_{fault\_per\_hr} \tag{A-13}$$

The constraint on $P_{md}[NSE_{V,fault\text{-}bias}]$ is then

$$P_{\mathrm{md}}\left[NSE_{V,\,fault-bias}\right] \begin{cases} \le \dfrac{10^{-9}}{P_{fault}} \text{ if } NSE_{V,\,fault-bias} > \left|E_{V\_safe\_\max}\right| \\ \le 1.0 \text{ if } NSE_{V,\,fault-bias} \le \left|E_{V\_safe\_\max}\right| \end{cases} \tag{A-14}$$

APPENDIX B: EFFECT OF A FAULT ON THE MEASUREMENT VECTOR

The effect of an error caused by a fault is taken into account in the following measurement vector equation in the Kalman filter.

$$z(k) = H(k)\cdot x(k) + v(k) \tag{B-1}$$

Suppose that a fault occurs on the j^{th} satellite some time prior to time t_k and causes a ramp error as shown below.

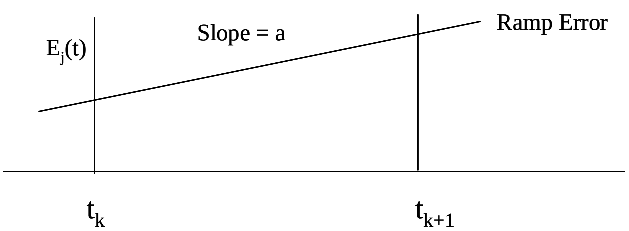

With PR measurements alone

$$E_j(k) = \frac{1}{dTk}\sum_{t=k\cdot dTk}^{(k+1)\cdot dTk} E_j(t) \tag{B-2}$$

$$dv_j(k) = \begin{bmatrix} 0 \\ \vdots \\ E_j(k) \\ \vdots \\ 0 \end{bmatrix} \tag{B-3}$$

In this case, $dv_j(k)$ is added to $v(k)$.

With both PR and delta PR measurements,

$$dv_j(k) = \begin{bmatrix} 0 \\ \vdots \\ E_j(k) \\ \vdots \\ E_{jr}(k) \\ \vdots \end{bmatrix} \tag{B-4}$$

where $E_{jr}(k)$ represents the effect of the fault on delta PR expressed as

$$E_{jr}(k) = \frac{1}{dTk}\sum_{t=k\cdot dTk}^{(k+1)\cdot dTk} \left(E_j(t) - E_j(t-1)\right)/\Delta t = a \tag{B-5}$$

In this case, $v(k)$ in (B-1) is changed to $v_j(k)$ where

$$v_j(k) = dv_j(k) + \begin{bmatrix} v_{PR}(k) \\ v_{DR}(k) \end{bmatrix} \tag{B-6}$$

Similar expressions can be derived for the step error.

APPENDIX C: VPL

This appendix derives VPL by extending the HPL formula developed for AIME by Dr. John Diesel [15]. AIME HPL is calculated as the root-sum-square of two parameters, which we call α_H and β_H. The derivation of these two parameters is explained below [14].

α_H is derived in a manner similar to that for RAIM HPL calculation. First, ramp errors of unit size starting at the previous cycle are emulated on each satellite, one at a time, and their effect on the position error and the test statistic is calculated. The maximum ratio of the position error and test statistic is then multiplied by a parameter known as pbias in RAIM to get α_H. The parameter pbias is the square root of the non-centrality parameter of the chi-square distribution that would make the probability of missed detection (P_{md}) of the assumed ramp error equal to 0.001. Derivation of α_H is discussed in detail in Dr. John Diesel's original paper in [15].

β_H is derived as

$$\beta_H = 5.33\sigma_H \tag{C-1}$$

where σ_H is the standard deviation of the horizontal position estimate uncertainty determined from the elements of the covariance matrix. The scalar 5.33 relates to the rare normal performance with a 10^{-7} probability.

Then

$$AIME\ HPL = \sqrt{\alpha_H^2 + \beta_H^2} \qquad \text{(C-2)}$$

Extending the formula to the vertical, VPL is given as

$$VPL = \sqrt{\alpha_V^2 + \beta_V^2} \qquad \text{(C-3)}$$

where α_V and β_V are the parameters for vertical corresponding to α_H and β_H respectively.

ACKNOWLEDGEMENTS

The authors would like to thank the FAA, particularly Bruce DeCleene, for supporting this work.

REFERENCES

1. Diesel, J. and J. King, “Integration of Navigation Systems for Fault Detection, Exclusion, and Integrity Determination—Without WAAS,” *Proceedings of The Institute of Navigation National Technical Meeting*, Anaheim, California, 18–20 January, 1995.

2. Brenner, M., “Integrated GPS/Inertial Fault Detection Availability,” *Proceedings of The Institute of Navigation 8th International Technical Meeting*, Palm Springs, California, September 1995.

3. Lee, Y. and S. Ericson, “Analysis of Coast Times Upon Loss of GPS Signals for Integrated GPS/Inertial Systems,” *Proceedings of The Institute of Navigation National Technical Meeting*, Anaheim, California, 22–24 January 2003.

4. GNSS Evolutionary Architecture Study (GEAS) Phase I Report, GEAS Panel, 24 January 2008.

5. Walter, T., et al., “Future Architectures to Provide Aviation Integrity,” *Proceedings of The Institute of Navigation National Technical Meeting*, San Diego, California, January 28–30, 2008.

6. Kovach, K., et al., ”GPS III Integrity Concept,” *Proceedings of The Institute of Navigation GNSS 2008*, Savannah, Georgia, 16–19 September 2008.

7. DeCleene B., et al., “Conceptual Framework for the Proposal for GBAS to Support CAT III Operations,” ICAO NSP/CSG/WP3, Toulouse, France,8–10 July 2008.

8. Murphy, T., “Development of Signal in Space Requirements for GBAS to Support CAT II/III Landing Operations,” *Proceedings of The Institute of Navigation GPS 2002*, Portland, Oregon, 24–27 September 2002.

9. Murphy, T., “Lower Level Monitor Requirements for GSL D,” ICAO NSP/WG1&2/WP64, Brussels, Belgium, 8–19 May 2006.

10. Shively, C., “Comparison of Methods for Deriving Ground Monitor Requirements for CAT IIIB LAAS,” *Proceedings of The Institute of Navigation National Technical Meeting*, San Diego, California, 22–29 January 2007.

11. Murphy, T., “Evolution of GBAS to Support CAT II/III Operations,” briefing to GNSS Evolutionary Architecture Study (GEAS) group, 29 January 2008.

12. Murphy, T., and M. Harris, “Geometry Screening for GBAS to Meet CAT III Integrity and Continuity Requirements” *Proceedings of The Institute of Navigation National Technical Meeting*, San Diego, California, 22–24 January 2007.

13. Hsiao, T., MITRE, private communication, 12 January 2007.

14. Lee, Y. and D. O’Laughlin, “Performance Analysis of a Tightly Coupled GPS/Inertial System for Two Integrity Monitoring Methods,” *NAVIGATION: Journal of the Institute of Navigation*, Vol. 47, No. 3, Fall 2000.

15. Diesel, J. and S. Luu, “GPS/IRS AIME: Calculation of Thresholds and Protection Radius Using Chi-Square Methods,” *Proceedings of The Institute of Navigation 8th International Technical Meeting*, Palm Springs, California, 12–15 September, 1995.

16. Memorandum from Daniel P. Salvano, Director, Navigation Services, FAA to IFOR Secretariat, 26 July 2004.

17. Clark, B. and B. DeCleene, “Alert Limits: Do We Need Them for CAT III?” *Proceedings of The Institute of Navigation GNSS 2006*, Fort Worth, Texas, 26–29 September 2006.